Dispersion Coefficient Prediction within a Bed Packed with Perfusive Particles

Bader H. Albusairi and James T. Hsu
Dept. of Chemical Engineering, Lehigh University, Bethlehem, PA 18015

DOI 10.1002/aic.10485
Published online March 30, 2005 in Wiley InterScience (www.interscience.wiley.com).

The effective medium model of perfusive particles has been used to modify the dispersion coefficient of a packed bed to account for intraparticle velocity and internal structure of the perfusive particles. In this model, the diffusivity factor has been derived by solving the steady-state diffusion equation in the three regions (that is, external, envelope, and internal regions) of the effective medium model and proved experimentally. The diffusivity factor is incorporated with hydrodynamic parameters obtained earlier to modify the dispersion coefficient of bed packed with perfusive particles. It was found that the diffusivity factor is independent of perfusive particle shape. Also, it was found that the uniformity of perfusive particles is not a necessary condition, once average accessible porosity is considered instead of actual porosity. Finally, it was shown that a significant error would be introduced to predict the performance of bed packed with perfusive particles if the effect of perfusive phenomena on the dispersion coefficient of a packed bed were not considered. © 2005 American Institute of Chemical Engineers *AIChE J,* 51: 1330–1338, 2005

Keywords: perfusive particle, intraparticle velocity, dispersion, effective diffusivity factor, effective medium model

Introduction

Chemical processes that use porous particles with interconnected pores (that is, perfusive particles) have emerged as a novel approach to solve the backpressure problems and low separation efficiency in packed beds such as HPLC.[1-4] This approach has shown a significant effect in reducing hot spots in exothermic reactors[5,6] and increasing the effectiveness factor for heterogeneous reactions.[7-10] The previous effects were explained by the presence of interconnected pores, which allowed heat and mass to transfer rapidly in, through, and out of perfusive particles by forced convection simultaneously with diffusion.

The enhancements accompanied by using perfusive particles as packing material have been recognized by previous studies of moment analysis,[2,4,11] numerical solution,[3,12,13] and discrete network modeling.[14] In these previous studies, the focus was only on the contribution of intraparticle flow on enhancing heat or mass transfer. Therefore, more attention has been focused on estimating intraparticle velocity to be used in heat and mass conservation equations.

Flow through permeable particles was initially discussed by Wheeler,[15] where a criterion for importance of intraparticle velocity was set. Unfortunately, a method of estimating intraparticle velocity was not provided. Intraparticle velocity was initially estimated as a fraction of column superficial velocity,[1,4,16] after which more advanced models such as the cell model,[17,18] the swarm model,[18] and the effective medium model[19] were proposed.

Researchers had focused on the contribution of intraparticle velocity on heat and mass transfer rates and they had not thoroughly studied the contribution of intraparticle convection on other system parameters such as mass transfer coefficient on the particle surface and column axial dispersion coefficient. These parameters were either estimated as having very large values arising from intraparticle convection or estimated based

Correspondence concerning this article should be addressed to J. T. Hsu at JTH0@lehigh.edu.

on conventional correlations. The enhancement of column axial dispersion coefficient attributed to the use of perfusive particles is investigated in this paper.

Dispersion of fluid flow in porous media is the occurrence and development of a transition zone between two domains of the fluid phase with different compositions. Dispersion is an effect of a combined action of both mechanical phenomena (such as velocity distribution) and physicochemical phenomena (such as diffusion), although the proper effect of each one cannot be distinguished.[20] In general, dispersion in porous media can be categorized according to its dependency on velocity into five different regimes: diffusion regime, superposition or transition regime, major mechanical or power-law regime, pure mechanical or convection regime, and turbulent regime.[20,21] Accordingly, the dispersion coefficient D_L is usually expressed in general as the sum of both mechanical and physicochemical phenomena,[20,22,23] as shown in Eq. 1, where Λ_e is the diffusivity factor defined as the ratio between the effective diffusivity within the perfusive medium and the absolute diffusivity in the unobstructed fluid; υ is the reduced velocity; U is the column superficial velocity; b_1 is the perfusive particle radius; D_{en} is the molecular diffusivity of the solute; and γ_2 and m are constants with values dependent on the dispersion regime

$$\frac{D_L}{D_{en}} = \Lambda_e + \gamma_2 \upsilon^m \qquad \upsilon = \frac{2Ub_1}{D_{en}} \tag{1}$$

The dispersion coefficient value depends on the geometrical structure of the porous medium (that is, porosity and permeability), characteristic of the fluid (that is, viscosity and density), and the characteristic of the displacement (that is, velocity distribution and distance traveled by transition zone).[20] Because using perfusive particles in packed beds would alter both the geometrical structure of the porous bed and the velocity magnitude and distribution, then a modification to the dispersion coefficient stemming from the use of perfusive particles is expected.

Geng and Loh[21] were the first to study the effect of perfusion on axial dispersion. They correlated the Knox equation and the power-law relationship to their experimental data. Geng and Loh[21] not only found that axial dispersion is the main reason for band broadening in perfusive chromatography, but also found that the extent of the velocity dependency of the axial dispersion is stronger in beds packed with perfusive particles than that in conventional diffusive packed beds, where this extent varies with pore size distribution and solute molecular size. These observations were expected, given that (1) interconnected pores in the perfusive particles added to the heterogeneity of the bed, by allowing the flow to pass through, and (2) pore size distribution controlled the particle permeability and, consequently, bed permeability.[18,19]

In this work, the focus will be on demonstrating the effect of intraparticle velocity and perfusive particle geometry on the column axial dispersion coefficient. To do that, a single proper model that represents both hydrodynamic and diffusive processes should be used. In the literature, few models have been proposed to predict the velocity profile inside and in the surroundings of the perfusive particle.[1,17,18] Unfortunately, a model that represents hydrodynamic processes very well is not necessary to be able to represent diffusive processes as well. It was found that different models resulted in different heat and mass transfer rates, whereas they predicted the same permeability.[24] Therefore, a proper model that adequately covers hydrodynamic and diffusive processes should be obtained.

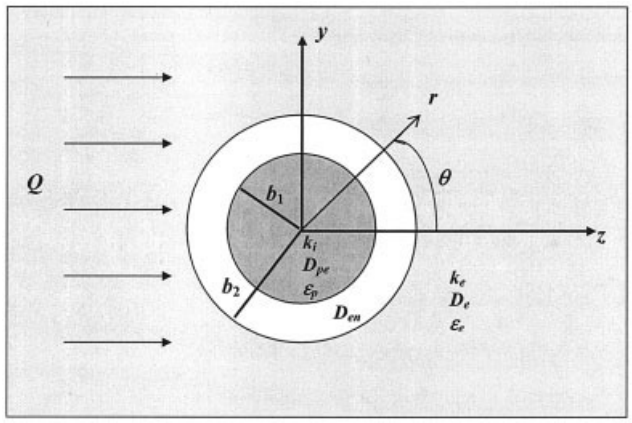

Figure 1. Effective medium model (EFMM).

The effective medium model (Figure 1) for impermeable particles, proposed by Neale and Nader[25] to represent diffusive processes and later also by Neale and Nader[26] to represent hydrodynamic processes, is a good candidate for adoption and modification. The effective medium model is a proper geometrical model for a bed packed with perfusive particles because it adequately represents hydrodynamic and diffusive flow processes in conventional packed beds.[24-28] Also, this model has been used because it was proposed by Hashin,[29] in estimating the effective properties of composite materials such as thermal conductivity, electrical conductivity, stress, strain, and thermal stresses,[30-33] in which the properties are equivalent to diffusive processes in porous media. In this field of science, the effective medium model is otherwise known as the general self-consistent scheme approximation. Recently, the effective medium model was modified by Albusairi and Hsu[19] to predict intraparticle velocity. The model was used to predict the enhancement on bed permeability when using perfusive particles with calculated intraparticle velocity (the results are shown in Figure 2); moreover, the model was validated experimentally.

In this article, an effective medium model will be adopted for permeable particles and used to estimate the axial dispersion coefficient by (1) estimating reduced velocity in a bed packed with perfusive particles, and (2) estimating the diffusivity factor Λ_e, theoretically and sequentially, to verify it experimentally. Finally, the importance of modifying the axial dispersion coefficient of a bed packed with perfusive particles will be explored.

Theory

Model description and velocity expressions

The effective medium model (Figure 1), is composed of a perfusive particle of radius, permeability, and an effective diffusivity of b_1, k_i, and D_{pe}, respectively. The perfusive particle is centered in a hypothetical envelope of radius and a diffusivity of b_2 and D_{en}, respectively. Both the envelope and the perfusive particle (that is, unit cell) are embedded in a

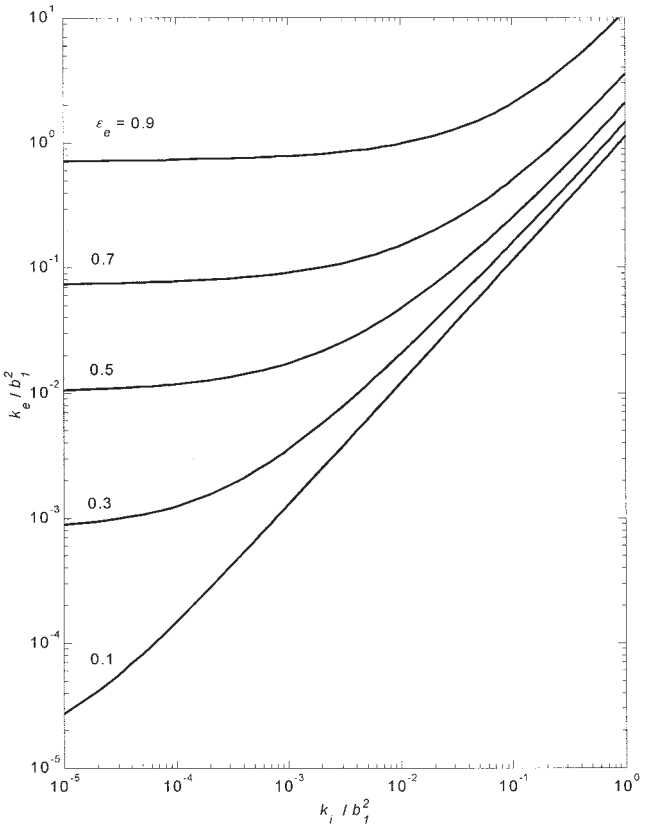

Figure 2. Perfusive bed permeability (k_e) as function of perfusive particle permeability (k_i) and external bed porosity ε_e.

Adopted from Albusairi and Hsu.[19]

porous medium of permeability and an effective diffusivity of k_e and D_e, respectively. The value of the envelope radius must satisfy the requirement that the total porosity of the unit cell equals the porosity of the external porous medium ε_e. Accordingly, the envelope radius b_2 will be calculated by Eq. 2. The perfusive particle is assumed to be composed of uniform impermeable spherical subparticles. Far from the envelope either a uniform superficial velocity of a magnitude U or a uniform mass flux of a magnitude Q is approaching the envelope. The former assumption has been used in estimating intraparticle velocity, whereas the latter assumption will be used in deriving the effective diffusivity factor Λ_e.

$$\lambda = \frac{b_2}{b_1} = (1 - \varepsilon_e)^{-1/3} \tag{2}$$

Albusairi and Hsu[19] assumed that the flow field in the envelope is governed by the Navier–Stokes equation, whereas the flow field in the external swarm of perfusive particles and the reference perfusive particle is governed by Brinkman's equation. Thus, the governed equations are

$$-\frac{\mu}{k_e}\mathbf{u}_e + \mu\nabla^2\mathbf{u}_e = \nabla P_e \qquad r > b_2 \tag{3}$$

$$\mu\nabla^2\mathbf{u}_{en} = \nabla P_{en} \qquad b_1 < r < b_2 \tag{4}$$

$$-\frac{\mu}{k_i}\mathbf{u}_i + \mu\nabla^2\mathbf{u}_i = \nabla P_i \qquad r < b_1 \tag{5}$$

$$\nabla \cdot \mathbf{u}_j = 0 \qquad j = e, en, i \tag{6}$$

In the above equations, $\mathbf{u}$ is the velocity vector; P is the pressure; μ is the viscosity; and the subscripts e, en, and i refer to external, envelope, and internal regions, respectively. Then they assumed the continuity of the pressure, the velocity vector, and the shear tensor throughout the proposed model as the model boundary. Using the stream function (ψ) method[26,34] to solve the proposed mathematical model, the following stream functions in the three model regions were obtained

$$\psi_e = \frac{Ub_1^2}{2\beta_e^2}\left[\frac{A_1}{\beta_e R} + B_2(\beta_e R)^2 + C_1\left(1 - \frac{1}{\beta_e R}\right)\exp(\beta_e R) + D_1\left(1 + \frac{1}{\beta_e R}\right)\exp(-\beta_e R)\right](\sin\theta)^2 \tag{7}$$

$$\psi_{en} = \frac{Ub_1^2}{2}\left(\frac{A_2}{R} + B_2 R + C_2 R^2 + D_2 R^4\right)(\sin\theta)^2 \tag{8}$$

$$\psi_i = \frac{Ub_1^2}{2\beta_i^2}\left\{\frac{A_3}{\beta_i R} + B_3(\beta_i R)^2 + C_3\left[\frac{\cosh(\beta_i R)}{\beta_i R} - \sinh(\beta_i R)\right] + D_3\left[\frac{\sinh(\beta_i R)}{\beta_i R} - \cosh(\beta_i R)\right]\right\}(\sin\theta)^2 \tag{9}$$

In the above equations, $\beta_e = b_1/k_e^{0.5}$; $\beta_i = b_1/k_i^{0.5}$; $R = r/b_1$; and A, B, C, and D are constants of integration. For detailed derivation and for the analytical expressions of the constants A, B, C, and D refer to Albusairi and Hsu.[19]

Derivation of the effective diffusivity factor Λ_e

Because of the assumption that the subparticles are impermeable, the imposed uniform mass flux is passing only through the interconnected pores of the perfusive particles. Moreover, because we are interested in the effective diffusivity, the fluid in the effective medium model will be assumed as stagnant. Accordingly, the following material balance of the proposed model can be adopted, where C_j refers to the solute concentration in the region represented by the subscript j

$$\mathbf{q}^j = -D_j\nabla C_j \qquad j = e, en, p \tag{10}$$

For steady state

$$\nabla \cdot \mathbf{q}^j = 0 \qquad j = e, en, p \tag{11}$$

Applying Eq. 11 in Eq. 10 will give the Laplace equation for the concentration in each of the regions (Eq. 12). The Laplace equation (Eq. 12), has a general solution shown in Eq. 13, where, values of F are constants of integration, R is the dimen-

sionless radial position, and P_n and Q_n are the nth-order Legendree polynomials of first and second kinds, respectively

$$\nabla^2 C_j = 0 \qquad j = e,\ en,\ p \tag{12}$$

$$C_j = \sum_{n=0}^{\infty} \{[F_{3n}R^n + F_{4n}R^{-(1+n)}][F_{1n}P_n(\cos\theta) + F_{2n}Q_n(\cos\theta)\} \qquad j = e,\ en,\ p \tag{13}$$

Because of z-axis symmetry, no mass flow is assumed to cross the z-axis along $\theta = 0$ and $\theta = \pi$ (Eq. 14). This boundary condition will set F_{2n} in Eq. 13 to 0 for all regions

$$q^j_\theta(r,\ 0,\ \phi) = q^j_\theta(r,\ \pi,\ \phi) = 0 \qquad j = e,\ en,\ p \tag{14}$$

The imposed uniform mass flux of magnitude Q at $r \to \infty$ set the boundary conditions for the concentration in the external region (Eqs. 15 and 16). Applying Eq. 15 to the developed relation of concentration in the external region would limit n to 0 and 1 because they are the only n values that give finite concentration at $r \to \infty$

$$q^e_r(\infty,\ \theta,\ \phi) = Q\cos\theta \tag{15}$$

$$q^e_\theta(\infty,\ \theta,\ \phi) = Q\sin\theta \tag{16}$$

Assuming continuous concentration profile, continuous mass flux at the interfaces, and finite concentration value at the center of the perfusive particle would give the following boundary conditions

$$q^e_r(b_2^+,\ \theta,\ \phi) = q^{en}_r(b_2^-,\ \theta,\ \phi) \tag{17}$$

$$q^{en}_r(b_1^+,\ \theta,\ \phi) = q^p_r(b_1^-,\ \theta,\ \phi) \tag{18}$$

$$C_e(b_2^+,\ \theta,\ \phi) = C_{en}(b_2^-,\ \theta,\ \phi) \tag{19}$$

$$C_{en}(b_1^+,\ \theta,\ \phi) = C_p(b_1^-,\ \theta,\ \phi) \tag{20}$$

$$C_p(0,\ \theta,\ \phi) = C_{po} \tag{21}$$

$$C^*_j = \frac{C_j - C_{po}}{C_e(r=\infty) - C_{po}} \qquad j = e,\ en,\ p \tag{22}$$

The concentration value at the center of the perfusive particle is an unknown finite value; to overcome this problem, a dimensionless concentration C^*_j, defined in Eq. 22, is used. Applying the above boundary conditions and dimensionless concentration, benefiting from the fact that there is no radial flux at $\theta = \pi/2$, would give the required equations to obtain the remaining constants of integration (that is, remaining F values).

According to the law of mass conservation, the mass flux magnitude in the unit cell must be equal to its value in the main stream (Eq. 23). Applying this equation to the obtained concentration profiles, and solving it for the diffusivity factor Λ_e, would give Eq. 24. The resulting equation for the diffusivity factor Λ_e (Eq. 24) is a modification to the result proposed by Neale and Nader[25] for impermeable particles (Eq. 25).

$$\pi b_2^2 Q = 2\pi \int_0^{b_1} q^p_\theta\left(r,\ \frac{\pi}{2}\right) r\,dr + 2\pi \int_{b_1}^{b_2} q^e_\theta\left(r,\ \frac{\pi}{2}\right) r\,dr \tag{23}$$

$$\Lambda_e = \frac{D_e}{D_{en}} = \frac{3\Lambda_p - 2(\Lambda_p - 1)\varepsilon_e}{3 + (\Lambda_p - 1)\varepsilon_e} \qquad \text{where } \Lambda_p = \frac{D_{pe}}{D_{en}} \tag{24}$$

$$\Lambda_e = \frac{2\varepsilon_e}{3 - \varepsilon_e} \qquad \text{if } \Lambda_p = 0 \text{ (impermeable particles)} \tag{25}$$

Using the assumption that the perfusive particle is a uniform spherical packed bed composed of impermeable subparticles and applying the result of Neale and Nader[25] for Λ_e (Eq. 25) on Λ_P would allow Λ_P to be expressed as in Eq. 26. Accordingly, Λ_e can be expressed as shown in Eq. 27, where ε_p is the porosity of the perfusive particle with respect to the perfusive channels only (that is, ε_p equals the volume of the interconnected channels divided by the total perfusive particle volume)

$$\Lambda_p = \frac{2\varepsilon_p}{3 - \varepsilon_p} \tag{26}$$

$$\Lambda_e = \frac{2[\varepsilon_e + (1 - \varepsilon_e)\varepsilon_p]}{3 - [\varepsilon_e + (1 - \varepsilon_e)\varepsilon_p]} \tag{27}$$

Dispersion coefficient correlation

The dispersion coefficient in a bed packed with perfusive particles will be estimated using Eq. 1 by adopting the effective medium model of perfusive particles. The effective diffusivity factor Λ_e will be estimated by Eq. 24 or Eq. 27, whereas the superficial velocity in the bed U of the uniform Darcy's flow will be estimated as shown in Eq. 28. The external pressure P_e in Eq. 28 will be estimated from the velocity expressions as predicted by the effective medium model. Moreover, bed permeability k_e will be estimated through Figure 2

$$\mathbf{U} = -\frac{k_e}{\mu}\nabla P_e \tag{28}$$

Perfusive particle permeability is either measured experimentally,[35] then modified later by Albusairi and Hsu[36] based on the shape factor, or estimated theoretically by using the Carmen–Kozeney equation (Eq. 29), as discussed in detail by Whitney et al.,[37] where b_{sp} is the diameter of the subparticle or the agglomerate of subparticles, depending on the perfusive particle structure used

$$\frac{k_i}{b_1^2} = \frac{\varepsilon_p^3}{150(1 - \varepsilon_p)^2}\left(\frac{b_{sp}}{b_1}\right)^2 \tag{29}$$

Experimental

Experimental setup and procedure

The electrical conductivity of a bed packed with perfusive particles will be measured experimentally and used to obtain, indirectly, the diffusivity factor Λ_e. The electrical conductivity is used because measuring the electrical conductivity is easier than measuring the diffusivity. Also, electrical conductivity results are less likely to be influenced by other factors such as natural convection. Furthermore, the results obtained from measuring the electrical conductivity can be applied to the molecular diffusivity.[25,38] Therefore, the basic experimental setup of Neale and Nader[25] has been adopted, as shown in Figure 3, to perform the conductance experiments for a bed packed with perfusive particles. The constructed electrical circuit (Figure 3A) consists of a conductance cell (C), a digital multimeter (Fluke 189) from Fluke Corporation (Everett, WA) (D), a signal generator (HP3301A) from Agilent Technologies (Palo Alto, CA) (S), and a 100-Ω resistance (R). The basic conductance cell is composed of a Plexiglas® tube bounded by two brass plates at each end (Figure 3B). The digital multimeter is used to measure the current passing through the conductance cell and the voltage drop across it. The signal generator is used to generate a 1000-Hz sine wave. Figure 4 shows the picture of the apparatus.

First, the conductance cell is filled with copper sulfate solution (4 g/L) as electrolyte and the conductance is measured. After that, the conductance cell is filled with the required type of perfusive particles and the electrolyte by gently shaking the cell to remove any trapped air in the particles and to ensure proper random packing. Then, the electrical conductance is measured, ensuring that the steady state has been reached. The electrical conductance of the cell, in which perfusive particles are present, is directly proportional to the external diffusivity (D_e) and the conductance of the cell filled with the electrolyte only is directly proportional to the molecular diffusivity (D_{en}).[25] Therefore, the division of any of the previous readings for different perfusive particles by the one obtained for pure electrolyte will give Λ_e.

Description of perfusive particles

Five types of perfusive particles, whose physical properties are listed in Table 1, were used in the series of experiments. Particle 1 (Figure 5A) is a spherical plastic particle with a single straight perfusive channel. Particle 2 (Figure 5B) is an acrylic cylindrical tube. Particle 3 (Figure 5C) is a hollow molded spherical plastic particle with uniformly distributed holes on its surface. Particle 4 (Figure 5D) is a hollow molded cylindrical plastic particle with uniformly distributed holes on its surface. Particle 5 (Figure 5E) is a plastic scrub cut into a box shape. Particles 3 and 4 are Jaeger Tri-Packs® and Jaeger rings, respectively (a gift from Jaeger Products, Inc., Houston, TX). Because a large quantity of perfusive particles of 10- to 100-micron diameter, having a defined internal structure and geometry, are not available commercially, slightly large diameter perfusive particles were selected for this study to evaluate the axial dispersion coefficients within a bed packed with perfusive particles.

Assuming the entire perfusive particle void is accessible to flux flow, then Λ_p can be estimated as shown in Eq. 26.

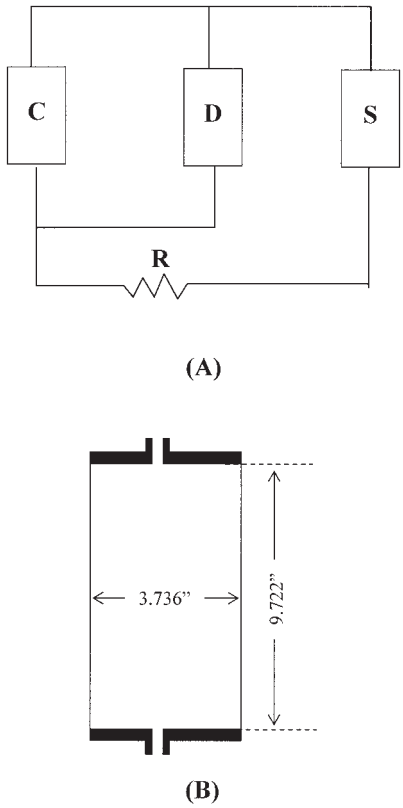

Figure 3. Experimental setup.

(A) Electrical circuit: C, conductance cell; D, digital multimeter; R, resistance; S, signal generator. (B) Conductance cell design.

With only a single perfusive channel in Particles 1 and 2, the void that is accessible to flux flow depends on the orientation of the particle in the packed bed; that is, if the perfusive channel is parallel to the flux then the entire void is accessible, whereas if it is perpendicular to the flux then no void is accessible to the flux. Because the perfusive particles will be packed randomly in the packed bed, then the average accessible void for flux flow $\varepsilon_{p,ac}$ will be equal to $\varepsilon_p \cos 45^\circ$ for Particles 1 and 2. Therefore, the accessible porosity $\varepsilon_{p,ac}$ will replace ε_p in all of the previous relations. For the remaining particles, the distribution of the channels, either on the surface or within the particle, is almost uniform and does not depend on the orientation; therefore $\varepsilon_{p,ac}$ will be identical to ε_p.

Results and Discussion

The observed behavior of the streamlines generated from the derived stream function equations of the effective medium model for a bed packed with perfusive particles (Eqs. 7–9), with changing perfusive particle permeability, is shown in Figure 6. This behavior indicates that more flow will pass through a bed packed with perfusive particles than that through a bed packed with conventional particles if they are subjected to the same pressure drop.

Theoretically, the derived equation for the diffusivity factor Λ_e (Eq. 24) satisfies its limiting cases, as observed from Figure 7. Experimentally, the shape and porosity of the perfusive

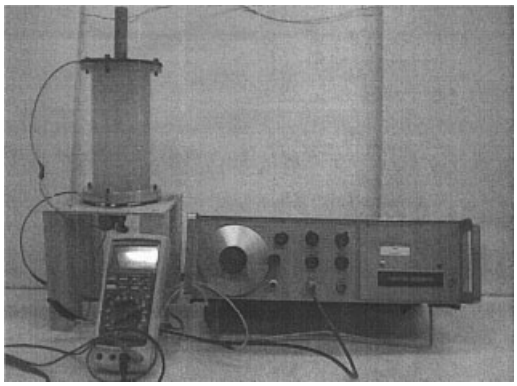

Figure 4. Apparatus used to perform conductance experiment.

particles were varied to examine the validity of the derived equation to predict the actual diffusivity factor Λ_e. Changing the shape of the perfusive particles allowed us to examine the sensitivity of the derived equation, especially that the derived equation depends on the volume fraction of the perfusive particles $(1 - \varepsilon_e)$. The theoretical predictions were in agreement with the experimental results, as shown in Table 2 and Figure 7. Therefore, the derived equation (Eq. 24) can be used for any perfusive particle regardless of the shape.

For the case of Particles 1 and 2, these particles were nonuniform, where only a single straight perfusive channel was available. Meanwhile, the derived equation for the diffusivity factor Λ_e (Eq. 27) was under the assumption of using a uniform perfusive particle. However, because the theoretical predictions were in agreement with the experimental results for Particles 1 and 2 when the porosity of the particles ε_p had been substituted by the accessible porosity of the perfusive particle $\varepsilon_{p,ac}$, then the derived equation (Eq. 27) can be used for any perfusive particle if the actual porosity is replaced by the accessible porosity.

Because the predictions of the diffusivity factor Λ_e and the superficial velocity U by the effective medium model for perfusive particles were proven experimentally, as shown above, then they can be used to modify the dispersion coefficient D_L, in Eq. 1, to accommodate the effect of using perfusive particles.

The following example will demonstrate the significant discrepancy to be introduced to the mass transfer in bed packed with perfusive particles if the perfusive effect is not considered.

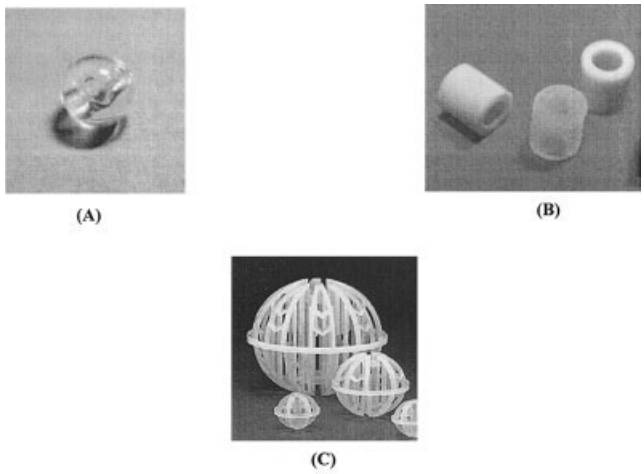

Figure 5. Perfusive particles used in the experiments.

(A) Particle 1, (B) Particle 2, (C) Particle 3, (D) Particle 4, and (E) Particle 5.

Assuming the correlation of the column axial dispersion coefficient was used without modifying the diffusive term and adopting the traditional correlations such as the Carmen–Kozeney equation to predict column permeability k_e and superficial velocity U, the predicted column axial dispersion coefficient for this case would accordingly be equal to the column axial dispersion coefficient for a bed packed with impermeable particles. Therefore, the ratio between the column axial dispersion coefficient of the bed packed with perfusive particles (D_L) to the assumed one in this example $(D_{L,imp})$ will be as shown in Eq. 30, where $\Lambda_{e,imp}$ is the diffusivity factor for a column packed with impermeable particles (Eq. 31) and U_{imp} is its superficial velocity, without considering the perfusive effect in its packed bed. The ratio U_{imp}/U in Eq. 30 was calculated from the effective medium model,[19] shown in Figure

Table 1. Particles Properties*

Particle Number	Dimensions	d_h	ε_p	$\varepsilon_{p,ac}$	Λ_p
1	$d_p = 0.61$ cm	0.16 cm	0.1026**	0.0725	0.0496
2	$L_p = 0.52$ cm	0.27 cm	0.3054**	0.2160	0.1551
	$R_p = 0.48$ cm				
3	$d_p = 2.54$ cm	—	0.90†	0.90	0.8571
4	$d_p = 1.60$ cm	—	0.86†	0.86	0.8037
5	$L_p = 1.30$ cm	—	0.77**	0.77	0.69
	$W_p = 1.20$ cm				
	$H_p = 0.85$ cm				

* d_h, diameter of the straight pore; d_p, perfusive particle diameter; H_p, height of perfusive particle; L_p, length of perfusive particle; R_p, radius of perfusive particle; W_p, width of perfusive particle; ε_p, total porosity of the perfusive particle; $\varepsilon_{p,ac}$, porosity of accessible channels in the perfusive particle; and Λ_p, perfusive particle diffusivity factor. (Λ_p from Eq. 26, $\varepsilon_{p,ac}$ for ε_p.)

**Measured by standard methods.

† Provided by manufacturer.

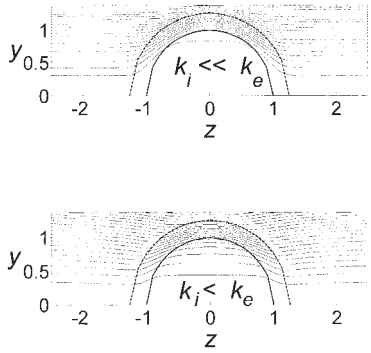

Figure 6. Stream lines generated by effective medium model for (A) perfusive particle with relatively low permeability, and (B) perfusive particle with relatively high permeability.

8, where the internal permeability of the particles k_i is assumed to be zero for U_{imp}, and the pressure drop is assumed identical for estimating U and U_{imp}. Figure 8 shows that the bed is packed more tightly (that is, ε_e decreases) as the perfusive effect on the superficial velocity becomes substantial. Thus, the discrepancy that would be introduced to the system if the perfusion effect were not considered in estimating the dispersion coefficient would be greater for beds packed tightly with perfusive particles, as observed from analyzing Eq. 30 and Figure 8

$$\frac{D_L}{D_{L,imp}} = \frac{\Lambda_e + \gamma_2 \upsilon^m}{\Lambda_{e,imp} + \gamma_2 \left(\frac{U_{imp}}{U}\right)^m \upsilon^m} \tag{30}$$

$$\Lambda_{e,imp} = \frac{2\varepsilon_e}{3 - \varepsilon_e} \tag{31}$$

To obtain the ratio $D_L/D_{L,imp}$ (as shown in Figure 9), the external porosity ε_e was set to 0.34, and the second coefficient γ_2 was set to 2.0, based on the experimental value reported by Carta et al.[2]; m was selected to equal 1.0, which was the primarily assumed value for porous media; and the perfusive particle radius b_1 and the subparticle radius b_{sp} were adopted from Whitney et al.[37] and set to 20 and 0.75 μm, respectively. As observed from Figure 9, the ratio $D_L/D_{L,imp}$ is higher for low υ values, where the dispersion coefficient was significantly enhanced by intraparticle convection compared to the one without it. Also, the ratio $D_L/D_{L,imp}$ becomes constant for $\upsilon > 5$, where the external convection term is the dominant one. Moreover, increasing the porosity of the interconnected pores in the perfusive particle ε_p will yield a higher $D_L/D_{L,imp}$ ratio, which is attributed to the contribution of the large perfusive effect accounted for in D_L and not in $D_{L,imp}$. This example illustrates the discrepancy that would be introduced to the system if the perfusion effect were not considered in estimating the dispersion coefficient, particularly if perfusive particles with high porosity are used.

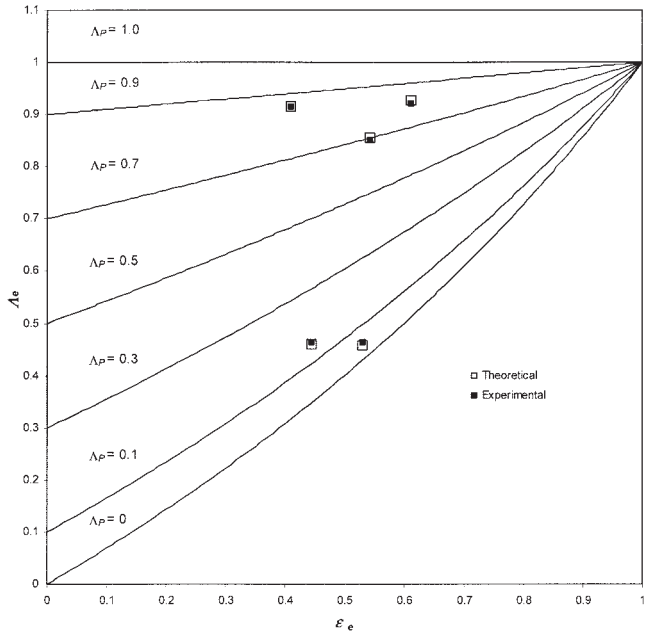

Figure 7. External diffusivity factor Λ_e, as function of ε_e and Λ_P.

Experimental results (■); corresponding theoretical results (□).

Finally, the diffusivity factor Λ_e can be extended to accommodate the case in which not all the pores in the perfusive particle are interconnected, as discussed by Whitney et al.,[37] and to accommodate the case in which the subparticles are permeable as assumed by Carta and Rodrigues[39] and Liapis et al.[40] For the first case, two porosities inside the perfusive particle will be considered: ε_p for the interconnected pores and ε_{pd} for the diffusive only pores. Then, mass transfer inside the perfusive particle can be assumed by two parallel mechanisms. The first mechanism is caused by the perfusion through the interconnected pores only, and the second mechanism is caused by the diffusion through the pores exhibit only diffusion. Accordingly, Eq. 24 for the diffusivity factor can be modified by substituting Λ_P by $\Lambda_{P,eff}$, which is defined by Eq. 32, where

Table 2. Experimental Results

Experiment Number	Media	ε_e *	Λ_e ** (Experimentally)	Λ_e † (Theoretically)	%Error
1	Particle 1	0.531	0.458	0.464	1.31
2	Particle 2	0.445	0.459	0.464	1.09
3	Particle 3	0.410	0.9137	0.914	0.03
4	Particle 4	0.613	0.9254	0.921	−0.475
5	Particle 5	0.544	0.8550	0.850	−0.585

* Measurement.
**Conductance of the cell without particles = 2.67×10^{-3} Ω^{-1}.
† Provided by Eq. 24, Λ_p from Table 1.

$\varepsilon_{pt} = \varepsilon_p + \varepsilon_{pd}$ and Λ_{pd} is the effective diffusivity in the pores exhibiting only diffusion divided by D_{en}

$$\Lambda_{p,eff} = \frac{\varepsilon_p}{\varepsilon_{pt}} \Lambda_p + \frac{\varepsilon_{pd}}{\varepsilon_{pt}} \Lambda_{pd} \tag{32}$$

For the second case, the perfusive particle can be considered as a bed packed with the subparticles. Therefore, the derived equation for the diffusivity factor in this work can be applied to estimate Λ_P, as shown in Eqs. 24 and 33, where Λ_{sp} is the diffusivity factor of the subparticles

$$\Lambda_p = \frac{3\Lambda_{sp} - 2(\Lambda_{sp} - 1)\varepsilon_p}{3 + (\Lambda_{sp} - 1)\varepsilon_p} \tag{33}$$

Finally, the proposed expressions for column axial dispersion coefficient predictions will allow simulation of heat and/or mass transfer problems more accurately. These problems may exist in heterogeneous catalytic reactions, particle removal in pollution control, microcarriers in animal tissue culturing, and bioparticles or cell separation.

Conclusion

The effect of using perfusive particles in packed beds on the column axial dispersion coefficient has been studied. The effective medium model for a bed packed with perfusive particles had been used to predict both the diffusive term and the convective term in the correlation of the column axial dispersion coefficient. First, the diffusive term of the dispersion coefficient (diffusivity factor, Λ_e) has been successfully derived and proved experimentally in this work for a bed packed with perfusive particles. From the experimental results it was found that Λ_e is independent of the perfusive particle shape and dependent on the perfusive particle volume fraction in the bed. Also, it was found that the uniformity of the perfusive particle is not necessary required and only the average accessible porosity is considered instead of actual porosity of the particle. Then, the effect of using information based on a bed packed with impermeable particles in estimating the dispersion coefficient in a bed packed with perfusive particles was evaluated. It was found that a significant discrepancy could be introduced to the system if the parameters are not properly estimated, especially for perfusive particles with high porosity. Finally, the diffusivity factor was extended to the case of bimodal perfusive particles where interconnected pores coexist with diffusive ones and to the case of permeable subparticles.

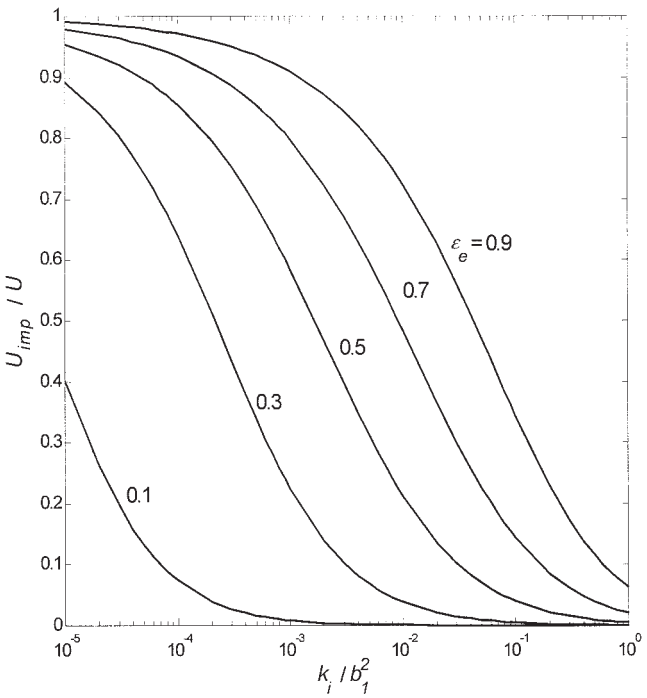

Figure 8. Ratio between superficial velocity of bed packed with impermeable particles (U_{imp}) and superficial velocity of bed packed with perfusive particles (U) as a function of bed external porosity (ε_e) and perfusive particle permeability (k_i), where the ratio is calculated by effective medium model assuming identical pressure drop.

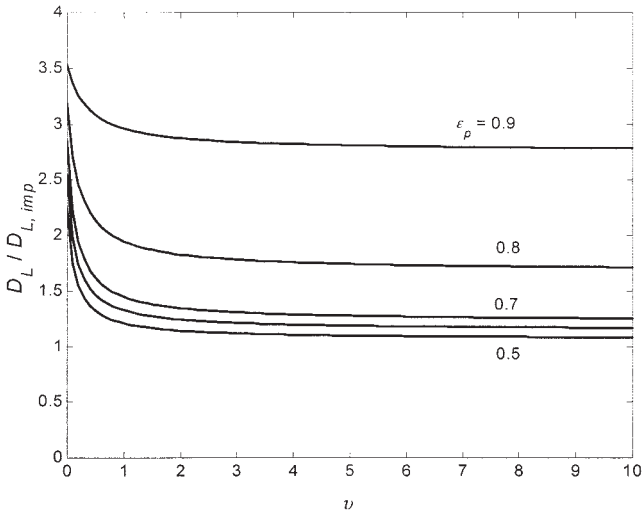

Figure 9. Ratio between dispersion coefficient of bed packed with perfusive particle (D_L) and dispersion coefficient of bed packed with impermeable particles ($D_{L,[infi]imp}$) as a function of particle porosity (ε_p) and reduced velocity (υ), where the ratio is estimated by the effective medium model.

ε_e = 0.34, b_1 = 20 μm, b_{sp} = 0.75 μm.

Acknowledgments

B. H. Albusairi thanks the Kuwaiti government for the scholarship from Kuwait University.

Notation

b_1 = perfusive particle radius
b_2 = envelope radius
b_{sp} = radius of subparticle
C = concentration
D = effective diffusivity
D_L = dispersion coefficient

k_e = packed bed permeability
k_i = perfusive particle permeability
P = pressure
P_n = nth-order Legendree polynomial of first kind (in Eq. 13)
Q = magnitude of mass flux at $r \rightarrow \infty$
q = mass flux
Q_n = nth-order Legendree polynomial of second kind (in Eq. 13)
$\mathbf{u}$ = velocity vector
U = superficial velocity

Greek letters

Λ = diffusivity factor
ε = void fraction (porosity)
λ = envelope dimensionless radius = b_2/b_1
μ = viscosity
υ = reduced velocity
ψ = velocity stream function

Subscripts and superscripts

e = external
eff = effective
en = envelope
i = internal or perfusive particle
imp = impermeable
O = origin ($R = 0$)
pd = diffusive pores
p = perfusive particle and interconnected pores for ε_p

Literature Cited

1. Afeyan NB, Gordon NF, Mazsaroff I, Varady L, Fulton SP, Yang YB, Regnier FE. Flow-through particles for the high-performance liquid chromatographic separation of biomolecules: Perfusion chromatography. *J Chromatogr A*. 1990;519:1-29.
2. Carta G, Gregory ME, Kirwan DJ, Massaldi HA. Chromatography with permeable supports: Theory and comparison with experiments. *Sep Technol*. 1992;2:62-72.
3. Liapis AI, McCoy MA. Theory of perfusion chromatography. *J Chromatogr*. 1992;599:87-104.
4. Rodrigues AE, Lopes JC, Lu ZP, Loureiro JM, Dias MM. Importance of intraparticle convection in the performance of chromatographic processes. *J Chromatogr A*. 1992;590:93-100.
5. Lopes JC, Dias MM, Mata VG, Rodrigues AE. Flow field and non-isothermal effects on diffusion, convection, and reaction in permeable catalysts. *Ind Eng Chem Res*. 1995;34:148-157.
6. Rodrigues AE, Ferreira RMQ. Effect of intraparticle convection on the steady-state behavior of fixed-bed catalytic reactors. *Chem Eng Sci*. 1990;45:2653-2660.
7. Nir A, Pismen LM. Simultaneous intraparticle forced convection, diffusion and reaction in a porous catalyst. *Chem Eng Sci*. 1977;32: 35-41.
8. Nir A. Simultaneous intraparticle forced convection, diffusion and reaction in a porous catalyst—II. Selectivity of sequential reactions. *Chem Eng Sci*. 1977;32:925-930.
9. Rodrigues AE, Lu ZP, Lopes JCB, Dias MM, Silva AM. The effect of intraparticle convection on conversion in heterogeneous isothermal fixed-bed reactors with large-pore catalysts for first-order reactions. *Chem Eng J Biochem Eng*. 1994;54:41-50.
10. Leitao A, Rodrigues A. Catalytic processes using "large-pore" materials: Effects of the flow rate and operating temperature on the conversion in a plug-flow reactor for irreversible first-order reactions. *Chem Eng J Biochem Eng*. 1995;60:111-116.
11. Rodrigues AE, Ahn BJ, Zoulalian A. Intraparticle-forced convection effect in catalyst diffusivity measurements and reactor design. *AIChE J*. 1982;28:541-546.
12. Ferreira RMQ, Almeida-Costa CA, Rodrigues AE. Effect of intraparticle convection on the transient behavior of fixed-bed reactors: Finite differences and collocation methods for solving unidimensional models. *Comput Chem Eng*. 1996;20:1201-1225.
13. Ferreira RMQ, Costa CA, Masetti S. Reverse-flow reactor for a selective oxidation process. *Chem Eng Sci*. 1999;54:4615-4627.
14. Meyers JJ, Liapis AI. Network modeling of the intraparticle convection and diffusion of molecules in porous particles packed in a chromatographic column. *J Chromatogr A*. 1998;827:197-213.
15. Wheeler A. Reaction rates and selectivity in catalyst pores. *Adv Catal*. 1951;3:250-337.
16. Komiyama H, Inoue H. Effects of intraparticle convective flow on catalytic reactions. *J Chem Eng Jpn*. 1974;7:281-286.
17. Neale G, Epstein N, Nader W. Creeping flow relative to permeable spheres. *Chem Eng Sci*. 1973;28:1865-1874.
18. Davis RH, Stone HA. Flow through beds of porous particles. *Chem Eng Sci*. 1993;48:3993-4005.
19. Albusairi BH, Hsu JT. Flow in beds packed with perfusive particles: Effective medium model for velocity prediction within the perfusive media. *Chem Eng J*. 2004;100:79-84.
20. Fried JJ, Combarnous MA. Dispersion in porous media. In: Chow VT, ed. *Advances in Hydroscience*. Vol. 7. New York, NY: Academic Press; 1971:169-282.
21. Geng A, Loh KC. Contribution of axial dispersion to band spreading in perfusion chromatography. *J Chromatogr A*. 2001;918:37-46.
22. Cussler EL. *Diffusion: Mass Transfer in Fluid Systems*. 2nd ed. New York, NY: Cambridge Univ. Press; 1997.
23. Wakao N, Kaguei S. *Heat and Mass Transfer in Packed Beds*. 1st ed. New York, NY: Gordon & Breach; 1982.
24. Wang W, Sangani AS. Nusselt number for flow perpendicular to arrays of cylinders in the limit of small Reynolds and large Peclet numbers. *Phys Fluids*. 1997;9:1529.
25. Neale GH, Nader WK. Prediction of transport processes within porous media: Diffusive flow processes within a homogeneous swarm of spherical particles. *AIChE J*. 1973;19:112-119.
26. Neale GH, Nader WK. Prediction of transport processes within porous media: Creeping flow relative to a fixed swarm of spherical particles. *AIChE J*. 1974;20:530-538.
27. Dodd TL, Hammer DA, Sangani AS, Koch DL. Numerical simulations of the effect of hydrodynamic interactions on diffusivities of integral membrane proteins. *J Fluid Mech*. 1995;293:147.
28. Li Y, Park C-W. Effective medium approximation and deposition of colloidal particles in fibrous and granular media. *Adv Colloid Interface Sci*. 2000;87:1-74.
29. Hashin Z. Assessment of the self consistent scheme approximation: Conductivity of particulate composites. *J Comp Mater*. 1968;2:284-300.
30. Boutin C. Microstructural influence on heat conduction. *Int J Heat Mass Transfer*. 1995;38:3181-3195.
31. Burr A, Monnerie L. On the stress, strain and energy density repartitions in particle-reinforced elastomer networks. *Polymer*. 2000;41: 5909-5919.
32. Sigl LS. Thermal conductivity of liquid phase sintered silicon carbide. *J Eur Ceram Soc*. 2003;23:1115-1122.
33. Vel SS, Batra RC. Three-dimensional analysis of transient thermal stresses in functionally graded plates. *Int J Solids Struct.* 2003;40: 7181-7196.
34. Bird RB, Stewart WE, Lightfoot EN. *Transport Phenomena*. 1st ed. New York, NY: Wiley; 1960.
35. Pfeiffer JF, Chen JC, Hsu JT. Permeability of gigaporous particles. *AIChE J*. 1996;42:932-939.
36. Albusairi B, Hsu JT. Application of shape factor to determine the permeability of perfusive particles. *Chem Eng J*. 2002;89:173-183.
37. Whitney D, McCoy M, Gordon N, Afeyan N. Characterization of large-pore polymeric supports for use in perfusion biochromatography. *J Chromatogr A*. 1998;807:165-184.
38. Schofield RK, Dakshinamurti C. Ionic diffusion and electrical conductivity in sands and clays. *Faraday Soc Discuss.* 1948;3:56.
39. Carta G, Rodrigues AE. Diffusion and convection in chromatographic processes using permeable supports with a bidisperse pore structure. *Chem Eng Sci.* 1993;48:3927-3935.
40. Liapis AI, Xu Y, Crosser OK, Tongta A. Perfusion chromatography: The effects of intra-particle convective velocity and microsphere size on column performance. *J Chromatogr A*. 1995;702:45-57.

Manuscript received Mar. 19, 2004, revision received Oct. 7, 2004, and final revision received Jan. 1, 2005.